JACS
JOURNAL OF THE AMERICAN CHEMICAL SOCIETY
Article
pubs.acs.org/JACS

Amphiphilic Molecular Motors for Responsive Aggregation in Water

Derk Jan van Dijken,[§,†] Jiawen Chen,[§,†] Marc C. A. Stuart,[†,‡] Lili Hou,[‡,†] and Ben L. Feringa*[,†]

[†]Centre for Systems Chemistry, Stratingh Institute for Chemistry, [‡]Groningen Biomolecular Sciences and Biotechnology Institute, University of Groningen, Nijenborgh 4, 9747 AG Groningen, The Netherlands

Supporting Information

ABSTRACT: The novel concept of amphiphilic molecular motors that self-assemble into responsive supramolecular nanotubes in water is presented. The dynamic function of the molecular motor units inside the supramolecular assemblies was studied using UV−vis absorption spectroscopy and cryo-transmission electron microscopy (cryo-TEM) microscopy. Reorganization between distinct, well-defined nanotubes and vesicles can be reversibly induced by light, going through the rotation cycle of the motor, i.e. driven by alternate photochemical and thermal isomerization steps in the system. This is the first example in which a molecular rotary motor shows self-assembly in an aqueous medium with full retention of its functionality, paving the way to increasingly complex, highly dynamic artificial nanosystems in water.

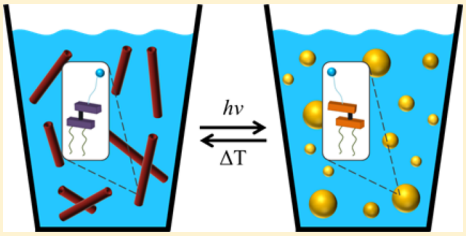

INTRODUCTION

Self-assembly of molecules into large and dynamic supramolecular structures is an imperative requirement for correct functioning of biological systems. Inspired by the fascinating examples of complex self-assembled structures created by Nature, the formation of well-defined nanoscale objects in water that are dynamic in nature and responsive to external stimuli has been a longstanding goal of many research groups.[1−3] The development of such artificial systems, in which molecular functions can be enhanced through cooperative effects in the self-assembled structures, and that can furthermore be visualized using electron microscopy, fluorescence, or scanning probe techniques, is a challenge that will bring artificial systems a step closer to advanced functions comparable to natural systems.[4−7] While supramolecular chemistry provides a great basis to increase complexity in a system, it is also intrinsically dynamic due to the labile nature of the interactions between the molecular units of the supramolecular assembly, making the design of and control over dynamic and responsive assemblies a daunting task.[8−10] Molecular self-assembly has therefore mainly focused on equilibrium systems, rather than systems that are far from equilibrium and, with great success, this has led to the design and development of a wide variety of functional molecules and supramolecular assemblies.[11] In addition to pushing the boundaries of functional systems by utilizing molecular self-assembly, such systems may lead to a better understanding of complex and dynamic processes found in Nature.[8] A key challenge in supramolecular chemistry is to gain full control over the assembly behavior, not only under thermodynamic equilibrium but also through synthetic design by introducing handles to control the morphology of the assemblies at will via external stimuli.

The concept of photoresponsive supramolecular assemblies, in which the morphology of self-assembled structures can be dynamically controlled by applying light as an external stimulus, has attracted much attention,[12] in part because material properties highly depend on the morphology of the (supra)-molecular constituents. Recent examples where photoresponsive building blocks have been employed to control morphology are most notably based on azobenzenes,[13−18] diarylethenes,[19−23] spiropyrans,[24−27] and photodimerizable moieties such as thymine or coumarin.[28−30] Often, photoresponsive systems only work in organic media, or by addition of organic solvent to aqueous solutions, and although examples of systems have been reported that work, or claim to work, in pure aqueous media,[30−34] or that influence the properties of water on an addressable surface,[35−37] their design and study is not trivial. This severely limits the comparison to natural systems as well as possibilities for biologically relevant applications. We envision that amphiphilic molecular motors which can be controlled with high precision by two orthogonal stimuli (light and heat) and have high photostationary states, hold great prospects for the development of responsive self-assembled systems in water in which well-defined supramolecular structures, e.g. nanotubes (Figure 1a), reorganize to give distinctly different self-assembled nano-objects, such as vesicles (Figure 1b), upon applying light as an external trigger. Moreover, given the fact that molecular motors, based on overcrowded alkenes, have multiple distinctly addressable states (isomers), we believe that the proof of concept provided in this work will lay the foundation for responsive, water-based systems with higher complexity than can be reached by photoswitches. Once the full potential of the rotary motor function can be harnessed it will allow adaptive and nonequilibrium behavior in self-assembled systems non-invasively powered by light.

Received: October 29, 2015
Published: December 23, 2015

DOI: 10.1021/jacs.5b11318
J. Am. Chem. Soc. 2016, 138, 660−669

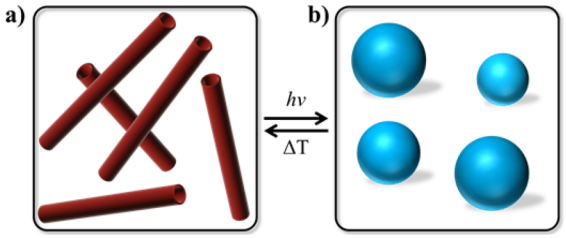

Figure 1. Schematic representation of envisioned changes in a supramolecular system upon isomerization of a self-assembled molecular motor constituent. (a) Nanotubes. (b) Vesicles. Interconversion between the two states is possible by photochemical and thermal isomerizations of the molecular motor.

Furthermore, the key characteristics of molecular motors should allow reformation of the original assemblies by applying heat as an orthogonal stimulus. Ideally, such a system is fully reversible and could be a major step to drive self-assembly out of equilibrium in aqueous media.

Light-driven molecular motors, based on overcrowded alkenes, can undergo isomerization around the central double bond, and the unidirectional rotary process has been used to dynamically control helical organization in liquid crystal films,[38] move nano- and microscale objects,[38,39] induce macroscopic contraction of gels,[40] and control catalytic function[41] and anion binding.[42] Important properties such as thermal stability (half-life) and rotation speed can be programmed by changing the molecular structure of the motor.[43−49]

Using the unique properties of molecular motors and utilizing their motion at the nanoscale to induce macroscopic changes in a system poses a significant challenge, and this concept is limited to a very few examples to date.[38,39] For instance, a molecular motor was employed to induce dynamic, helical organization in a liquid-crystal film, and the rotation of the motor, and subsequent reorganization of the liquid-crystal film, could be used to move a micrometer-sized glass rod, placed on top of the film.[38] Molecular motors show promise for the development of sophisticated molecular machines and increasingly complex systems, and recent developments show how attaching molecular motors to surfaces, or by letting them operate at interfaces, are promising strategies to exploit the dynamic properties of the motor functionality.[35,36,50−52]

Herein we report a unique system that shows responsive assembly in water, based on amphiphilic rotary molecular motors that form well-defined tubular aggregates. These highly dynamic nanotubes undergo reversible morphological changes when going through the rotary cycle of the molecular constituent and alternating between light and heat as external stimuli cause on-demand reorganization of the nanotubes to vesicles and *vice versa* as schematically shown in Figure 1.

In the four-step rotary cycle (Scheme 1), the steric crowding around the central tetrasubstituted alkene bond (the rotary axle) forces the molecule to adapt a nonplanar shape in order to minimize the steric repulsion. In the stable *trans* isomer, the substituent at the stereogenic center (Me-group in Scheme 1) adopts a pseudo-axial conformation. Upon photochemical isomerization from the stable *trans* to the unstable *cis* isomer (Scheme 1, step 1), the Me-substituent adopts an unfavored pseudo-equatorial orientation. Upon heating (Scheme 1, step 2), the unstable *cis* isomer can undergo a thermal helix inversion to form the stable *cis* isomer, releasing the conformational strain as the stereogenic methyl moiety adopts again a pseudo-axial conformation. Starting from stable *cis*, the

Scheme 1. Unidirectional Rotary Cycle of a Molecular Motor[a]

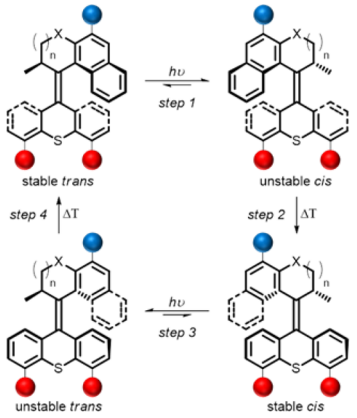

[a]Spheres indicate the connecting positions for the hydrophilic (blue) and hydrophobic (red) moieties.

photochemical (Scheme 1, step 3) and thermal (Scheme 1, step 4) steps complete the 360° rotation cycle via the unstable *trans* isomer.[53,54] An important feature of these molecular motors is the irreversibility of the thermal isomerization steps that ensures that the rotation of the upper-half of the molecular motor, with respect to the lower-half, is unidirectional,[55] and this unidirectional nature of the rotary process has been demonstrated by NMR and CD spectroscopy[48,54] and supported by theoretical calculations.[55]

As our approach described here is the first example in which a molecular motor was designed to self-assemble into supramolecular aggregates in water, retention of functionality of the motor constituent in the aggregates was a key challenge. Light-induced isomerization might sterically affect the neighboring amphiphilic motor molecules in the aggregate and therefore likely be unfavorable. Additionally, other processes, such as inter- or intramolecular photochemical reactions and energy or electron transfer, might occur when the motors are in close proximity to each other while aggregated.[56−58]

RESULTS AND DISCUSSION

Design. The approach described here aims to enhance the motor's properties through cooperative self-assembly. To date, the functioning of molecular motors in water has not been demonstrated, however, nor are there, to the best of our knowledge, any examples of artificial self-assembling motors. We therefore designed two amphiphilic molecular motors that were expected to have relatively short (**1**) and long (**2**) half-lives, respectively (Figure 2).[44,59] Motor **1** constitutes a five-membered cyclopentene upper-half and **2** bears a six-membered dihydrothiopyran upper-half. For the proof of principle described in the work presented here, amphiphilic molecular motors **1** and **2** have a symmetric lower-half. Therefore, the stable *trans* and *cis* isomers (henceforth referred to as "stable"), as well as the unstable *trans* and *cis* isomers (henceforth referred to as "unstable"), are identical.

The light-responsive overcrowded alkene core connects two hydrophobic dodecyl tails with a hydrophilic charged quaternary ammonium moiety that is attached to the aromatic core through an ethylene glycol linker.

The design of molecular motors **1** and **2** is based on our previously reported system, in which bis-thioxanthylidene

DOI: 10.1021/jacs.5b11318
J. Am. Chem. Soc. 2016, 138, 660−669

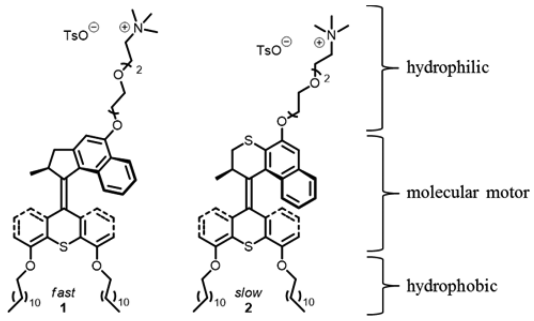

Figure 2. Design and structure of amphiphilic molecular motors **1** (fast) and **2** (slow).

amphiphiles, connected through a tetrasubstituted alkene bridge, formed nanotubes in water.[60] We showed that the nanotubes could be photochemically disassembled through a ring-closing reaction. This process is, however, irreversible,[60,61] limiting its attractiveness for the development of new responsive supramolecular systems. Employing a highly reversible system, based on molecular motors **1** and **2**, which can undergo photochemical and thermal steps in a fully controlled manner, we reasoned that reversible changes in morphology might be possible. In the design of molecular motors **1** and **2**, the lower-half was kept identical to that of the previously reported bis-thioxanthylidene amphiphiles,[60] as we could attribute the formation of nanotubes to the tight packing of the hydrophobic moiety, which makes up the internal part of the bilayers. Based on this structural motif (Figure 2), we predicted that self-assembly of molecular motors **1** and **2** in water would be facile. The hydrophilic moiety in the upper-half was introduced along the same axis as the hydrophobic moiety, and to ensure bilayer formation over the formation of other assemblies, the single ethylene glycol chain was enlarged through functionalization with a charged trimethylammonium moiety in order to keep the packing parameter close to 1.[60,62−64] Upon applying an external stimulus, morphological changes might occur in the nano-objects due to changes in the shape of the motor[38] or the movement of the molecular components[39] in the self-assembled objects.

Synthesis. The key step in the synthesis of amphiphilic motors **1** and **2** is the formation of the central, overcrowded olefinic bond. The diazo-thioketone coupling[65,66] is commonly applied for the synthesis of this type of sterically demanding alkenes, allowing the coupling of distinct upper and lower halves and thereby building the framework of the molecular motor.[48,54] The required building blocks for the olefin formation are a thioketone and a hydrazone, both of which are usually prepared from the corresponding ketone precursors. The hydrophobic precursor **7** (upper-half) of fast motor **1** was prepared starting from 1-methoxynaphthalene (Schemes 2 and S1 in the Supporting Information).

Upon reaction with methacrylic acid, a one-pot Friedel−Crafts acylation and subsequent Nazarov cyclization afforded **3** in 45% yield over the two steps. Deprotection of the phenol moiety with pyridine hydrochloride gave **4** which reacts with monotosyl-tri(ethylene glycol) **5** to give **6**. The ethylene glycol OH was then protected with TBDPS-Cl in the presence of imidazole to yield upper-half ketone **7**.

Ketone **14** was synthesized in six steps according to a procedure recently reported by our group[60] and is described in detail in the Supporting Information (Schemes S2−S3). To

Scheme 2. Synthesis of the Hydrophilic Precursor of the Upper-Half Ketone 7 of Fast Motor 1[a]

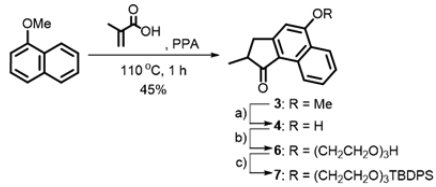

[a]Reagents and conditions: (a) pyridine hydrochloride (21 equiv), 190 °C, 2 h, 78%; (b) $TsO(CH_2CH_2O)_3H$ **5** (1.1 equiv), Cs_2CO_3 (3.0 equiv), DMF, reflux, 16 h, 68%; (c) TBDPS-Cl (1.5 equiv), imidazole (5.0 equiv), DMF, reflux, 12 h, 75%.

increase its reactivity for the subsequent olefination step, ketone **14** was transformed into the corresponding thioketone with Lawesson's reagent (Scheme 3). Thioketone **15** was

Scheme 3. Synthesis of Amphiphilic, Fast Molecular Motor 1[a]

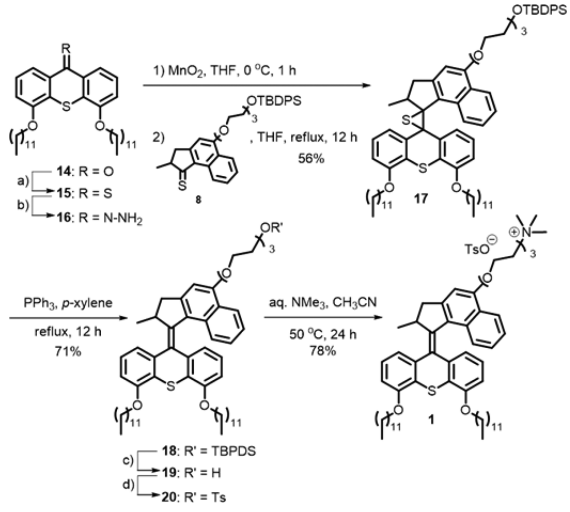

[a]Reagents and conditions: (a) Lawesson's reagent (3.0 equiv), toluene, reflux, 30 min, quant; (b) aq. NH_2NH_2 (39 equiv), THF, RT, 10 min, quant; (c) TBAF (1.1 equiv), THF, 0 °C, 1 h, 95%; (d) TsCl (2.7 equiv), NEt_3 (160 equiv), CH_2Cl_2, RT, 16 h, 72%.

converted into hydrazone **16** with hydrazine monohydrate in quantitative yield. *In situ* oxidation of **16** with MnO_2 at 0 °C, followed by addition of freshly prepared thioketone **8** in THF, yielded episulfide **17**. Desulfurization of episulfide **17** with PPh_3 gave sterically demanding alkene **18**, which was deprotected using TBAF (**19**) and subsequently converted into tosylate **20** with TsCl. Reaction of **20** with aq. NMe_3 gave cationic amphiphile **1**, bearing TsO^- as the counterion. After optimizing the synthesis of amphiphilic molecular motor **1**, molecular motor **2** was prepared using a similar strategy (Schemes 4, 5).

Deprotonation of 2-methoxynaphthalene with *n*-BuLi and quenching with elemental sulfur (S8) gave thiol **21**. Conjugate addition with methacrylic acid yielded **22**, which was converted into the corresponding acid chloride with oxalyl chloride, followed by Friedel−Crafts acylation in the presence of $AlCl_3$ to provide **23**. Using a similar protocol as shown in Scheme 2, deprotection of the phenol moiety of **23** with pyridine hydrochloride gave **24**, which reacts with monotosyl-tri-(ethylene glycol) **5** to give **25**. The ethylene glycol OH was then protected with TBDPS-Cl in the presence of imidazole.

DOI: 10.1021/jacs.5b11318
J. Am. Chem. Soc. 2016, 138, 660−669

Scheme 4. Synthesis of the Hydrophilic Precursor of the Upper-Half Hydrazone 27 of Slow Motor 2[a]

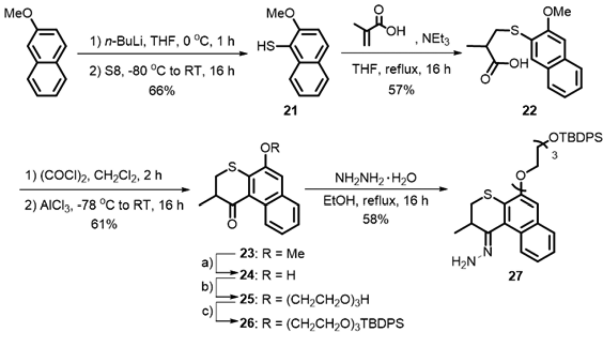

[a]Reagents and conditions: (a) pyridine hydrochloride (26 equiv), 190 °C, 2 h, used without purification; (b) $TsO(CH_2CH_2O)_3H$ **5** (1.1 equiv), K_2CO_3 (3.0 equiv), DMF, 90 °C, 16 h, 68%; (c) TBDPS-Cl (1.5 equiv), imidazole (5.0 equiv), DMF, 95 °C, 15 h, 75%.

Scheme 5. Synthesis of Amphiphilic, Slow Molecular Motor 2[a]

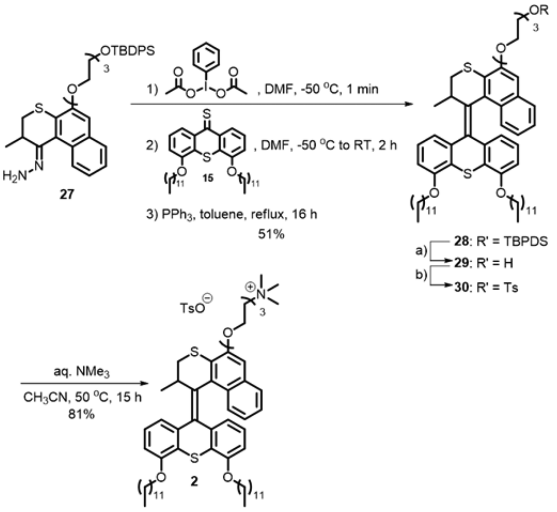

[a]Reagents and conditions: (a) TBAF (1.1 equiv), THF, 0 °C, 1 h, 91%; (b) TsCl (1.9 equiv), NEt_3 (112 equiv), CH_2Cl_2, RT, 16 h, 78%.

Finally, ketone **26** was transformed into the corresponding hydrazone **27** with hydrazine monohydrate.

Hydrazone **27** was converted to its diazo derivative by oxidation with diacetoxyiodobenzene in DMF at −50 °C, followed by the addition of thioketone **15** in DMF. The reaction mixture was allowed to warm to room temperature during 2 h to yield the episulfide which was converted into overcrowded alkene **28** using PPh_3 in 51% yield over the three steps. Deprotection of the alcohol group with TBAF gave **29** in high yield. After conversion to the corresponding tosylate and subsequent reaction with aq. NMe_3, slow molecular motor **2** was obtained in 81% yield. Amphiphilic motors **1** and **2** were characterized by ^1H and ^{13}C NMR, UV−vis absorption spectroscopy, and HRMS (see Supporting Information), and photochemical and thermal isomerization processes were compared with those of their parent motor structures.[46,49,67,68]

Self-Assembly and Morphology. With both molecular motors in hand, aggregation of **1** and **2** was first confirmed by cryo-transmission electron microscopy (cryo-TEM).[69] The charged quaternary ammonium group ensures water solubility, and we found that, for motors **1** and **2**, bearing a simple triethylene glycol chain, the corresponding amphiphiles (**19** and **29**) are not soluble enough to give any well-defined aggregation in water. Pure **1** or **2** did not give well-defined structures, and only small pieces of bilayer could be observed. Previous work from our group has shown that the addition of phospholipids can increase the tendency of amphiphiles to form well-defined self-assembled structures.[60] Addition of 1,2-dioleoyl-*sn*-glycero-3-phosphocholine (DOPC) in a 1:1 ratio (see Supporting Information for details) indeed led to the formation of nanotubular structures for both **1** and **2** (Figure 3). DOPC alone forms vesicles upon self-assembly in water,[70] and further control experiments are discussed later and in the Supporting Information.

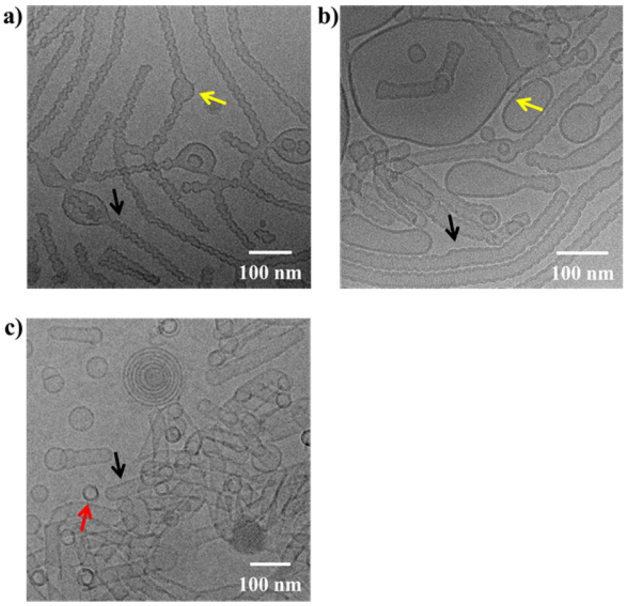

Figure 3. Cryo-TEM microscopy images of (a) coassemblies of amphiphile **1** and DOPC (ratio 1:1). (b) Extruded (pore size 200 nm) coassemblies of amphiphile **1** and DOPC (ratio 1:1).[71] (c) Coassemblies of amphiphile **2** and DOPC (ratio 1:1).[72] Samples are in water, and the total concentration of amphiphile is 1 mg/mL. Black arrows indicate nanotubes in the specimen plane; yellow arrows indicate DOPC bilayers; red arrows indicate nanotubes perpendicular ("standing up") to the specimen plane.

Cryo-TEM analysis shows that **1** forms tubular structures when coassembled with DOPC in a 1:1 ratio (Figure 3a). The tubes are several micrometer in length and have a diameter of 15−25 nm, with a typical bilayer wall of approximately 4 nm thick. A phase separation is observed between the DOPC lipid bilayers and the tubular structures formed by amphiphilic motor **1** (Figure 3a−b; yellow and black arrows, respectively). The DOPC vesicles and stretched vesicles have a smooth bilayer (indicated with yellow arrows in Figure 3a−b) whereas the tube-like aggregates of amphiphilic motor **1** have uneven, "toroidal" bilayer walls (indicated with black arrows in Figure 3a−b). Although the diameter differs to some extent (15−25 nm) from tube to tube, within the same tube the assembly is generally homogeneous. While twisted nanotubes have been reported as intermediates in the formation of regular, straight nanotubes,[63,73] to the best of our knowledge there is no literature precedence for toroidal nanotubular structures such as observed from self-assembly of **1**. While amphiphile **2** also

DOI: 10.1021/jacs.5b11318
J. Am. Chem. Soc. 2016, 138, 660−669

assembles with DOPC (ratio 1:1) and forms straight tubular structures in water (Figure 3c,[72] black arrows indicate nanotubes in the specimen plane; red arrows indicate nanotubes perpendicular to the specimen plane), the morphology is different from the aggregates formed by motor **1**. The tubes are much shorter and typically 100−200 nm in length, with a diameter of 30 nm. When the amount of DOPC is decreased (ratio **2**/DOPC is 4:1), or increased (ratio **2**/DOPC is 1:4), identical nanotubes are formed as in the 1:1 mixtures. These results indicate that DOPC stimulates aggregate formation, but does not play a further role in the morphology of the self-assembled amphiphilic motor but phase separates. Further experiments were carried out with 1:1 mixtures of **2** and DOPC.

Photochromic Properties. After confirming that well-defined tubular aggregates are formed from both **1** and **2**, albeit with different morphology, the photochemical properties and functioning of the molecular motors **1** and **2** were studied using UV−vis absorption spectroscopy. Both organic solutions of **1** (Figure 4a) and **2** (Figure 4c), as well as self-assembled

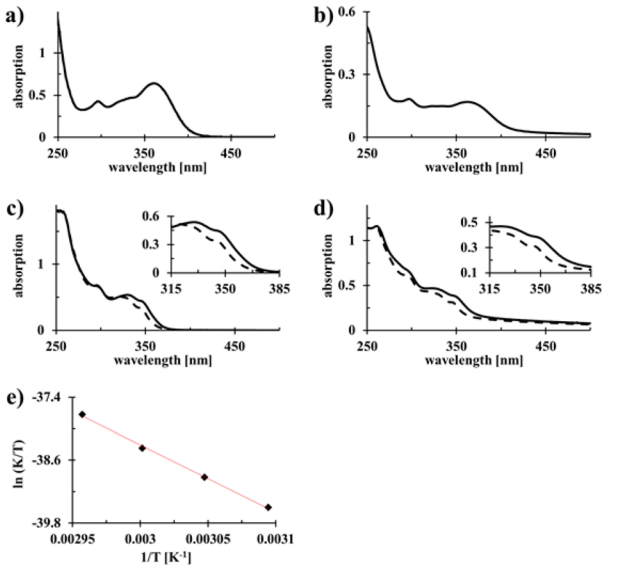

Figure 4. UV−vis absorption spectra. (a) Solution of **1** in MeOH (2.5×10^{-6} M) before and after irradiation (10 min, λ_{irr} = 365 nm). (b) Nanotubes of **1** with DOPC (1:1) in water (1 mg/mL) before and after irradiation (10 min, λ_{irr} = 365 nm). (c) Solution of **2** in CH_2Cl_2 (2.5×10^{-6} M) before (solid line) and after (dashed line) irradiation (2 h, λ_{irr} = 365 nm). (d) Nanotubes of **2** with DOPC (1:1) in water (1 mg/mL) before (solid line) and after (dashed line) irradiation (10 min, λ_{irr} = 365 nm). (e) Eyring plot for the thermal helix inversion of unstable **2** to stable **2**. Spectra before and after irradiation in (a) and (b) overlap. Insets in (c) and (d) are expanded areas of λ = 315−385 nm.

nanotubes of these amphiphiles in water (Figure 4b and 4d, respectively), showed the typical absorption spectra for molecular motors of these types.[46,67]

Unfortunately, for fast molecular motor **1**, no changes in absorption were observed (Figure 4a−b), independent of the irradiation time (confirmed for up to 2 h, λ_{irr} = 365 nm), neither in methanol solution (Figure 4a) nor aqueous solution containing the self-assembled nanotubes (Figure 4b). We postulated that molecular motor **1** might revert from unstable **1** to stable **1** too fast to detect spectral changes with our standard setup. To probe this hypothesis, transient absorption measurements were conducted. Upon 355 nm pulsed excitation of stable **1**, the absorption immediately increased at λ = 430 nm and decreased at λ = 350 nm, and the decay trace showed complete recovery within 160 μs in isopentane at 173 K (Figure 5a).

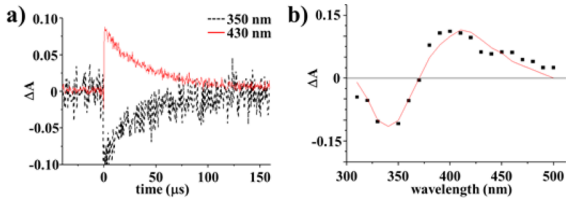

Figure 5. Transient decay and recovery following pulsed excitation of **1** in isopentane at 173 K. (a) At λ = 350 nm (black striped line) and λ = 430 nm (red solid line). (b) UV−vis difference spectrum 100 ns after excitation.

Fitting with a single exponential, a lifetime of 47 μs at 173 K was determined. The UV−vis absorption difference spectrum of **1** at 100 ns after excitation (Figure 5b) indicates that the absorption band between λ = 300−375 nm decreases and a new band between λ = 375−500 nm appears upon photoisomerization. The change in absorption spectra upon irradiation is similar to that observed for related molecular motors of this type of core structure.[43,48,53,54] Next, rate constants of the thermal isomerization step of unstable **1** to stable **1** were determined at six different temperatures (168, 173, 178, 183, 188, and 193 K) by following the transient recovery at 430 nm (Figure 6a−c). Using the Eyring equation,

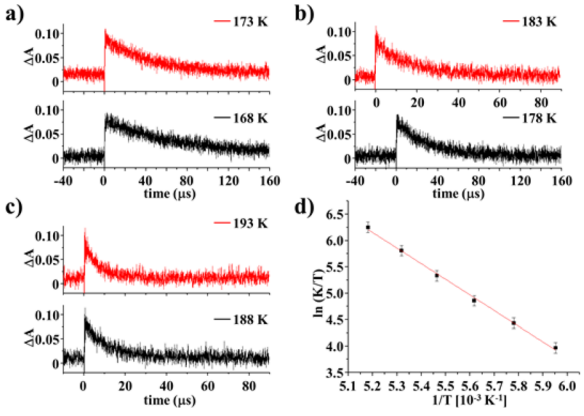

Figure 6. Transient recoveries for **1** (at λ = 430 nm, in isopentane) upon pulsed irradiation at λ = 355 nm at various temperatures. (a) 168 K; 173 K. (b) 178 K; 183 K. (c) 188 K; 193 K. (d) Eyring plot for the thermal helix inversion of unstable **1** to stable **1**.

the Gibbs free energy of activation ($\Delta^{\ddagger}G^{\circ}$) was calculated as 29.6 ± 0.5 kJ/mol corresponding to a half-life ($t_{1/2}$) of around 40 ns at 20 °C. Furthermore, the enthalpy of activation and entropy of activation were calculated: $\Delta^{\ddagger}H^{\circ}$ = 24.6 ± 0.5 kJ/mol and $\Delta^{\ddagger}S^{\circ}$ = −18.3 ± 0.5 J/mol·K, and these data are in agreement with data obtained for molecular motors with a similar upper half.[46,49]

With the rate of thermal helix inversion at 20 °C being 2.0×10^7 s^{-1}, molecular motor **1** is capable of achieving unidirectional rotation at 10 MHz at room temperature under suitable irradiation conditions. This makes **1** one of the fastest light-driven molecular motors of this type.[48] The high rotation speed

DOI: 10.1021/jacs.5b11318
J. Am. Chem. Soc. 2016, 138, 660−669

of **1** explains why the absorption spectrum in solution does not show any change upon irradiation, confirming our hypothesis that unstable **1** isomerizes back to stable **1** before the absorption spectrum can be measured using standard equipment. In addition, cryo-TEM did not reveal any changes in morphology upon irradiation or heating of nanotubes of stable **1** (Figure 7), indicating that either the motor does not

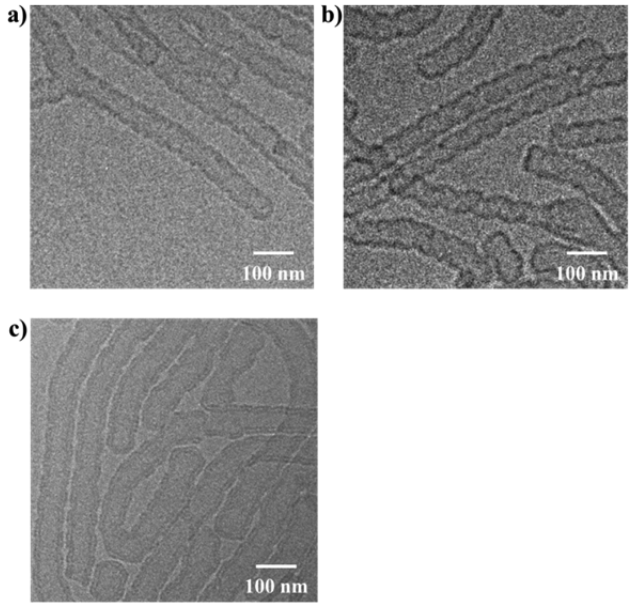

Figure 7. Cryo-TEM microscopy images of coassemblies of amphiphile **1** and DOPC (1:1) in water at a total concentration of 1 mg/mL. The consecutive processes are (a) before irradiation; (b) after irradiation (10 min, λ_{irr} = 365 nm); (c) heated at 60 °C for 1 h.

isomerize while aggregated or the state of the motor (stable versus unstable) has no influence on the aggregation. Alternatively, reorganization of the aggregates may be slower than the isomerization of the molecular motor.

Much to our delight, however, upon irradiation of slow molecular motor **2** in CH_2Cl_2 solution (2 h, λ_{irr} = 365 nm), the spectrum shows a hypsochromic shift (Figure 4c, solid to dashed line), in accordance with isomerization of the stable to the unstable isomer of the previously studied unfunctionalized molecular motor analog.[46,67,68] The rate constants of the thermal isomerization step of unstable **2** to stable **2** were determined at four different temperatures (50, 55, 60, and 65 °C) by following the decrease in absorption at 312 nm (Figure 4e; for details, see Supporting Information Figure S49). Using the Eyring equation, the Gibbs free energy of activation ($\Delta^{\ddagger}G°$) was calculated as 106.2 kJ/mol corresponding to a half-life ($t_{1/2}$) of around 270 h at 20 °C and 4.30 h at 50 °C. Furthermore, the enthalpy of activation and entropy of activation were calculated: $\Delta^{\ddagger}H°$ = 106.7 kJ/mol and $\Delta^{\ddagger}S°$ = 1.6 J/mol·K. Note that the entropy term for slow motor **2** is positive, while for fast motor **1** it was negative (see above). We propose that this is due to a different transition state during the thermal helix inversion step as **1** and **2** bear different upper halves (5- versus 6-membered ring), which consequently leads to a difference in the change in volume upon isomerization from the unstable to the stable isomer. The obtained entropy values are in good agreement with previously determined values for similar (nonamphiphilic) molecular motors.[48,49]

In addition to UV−vis absorption spectroscopy, ^{1}H NMR was employed to confirm the isomerization of stable **2** to unstable **2** in solution (Figure 8). After irradiation with UV

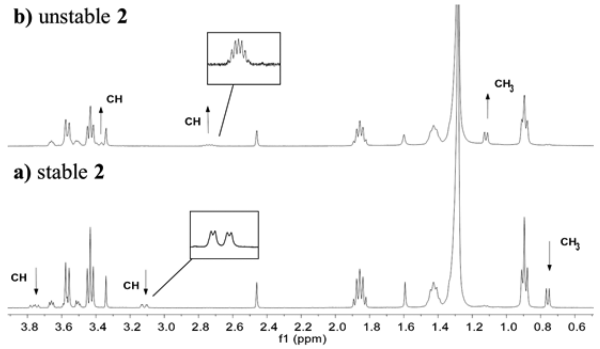

Figure 8. Partial ^{1}H NMR spectra of (a) stable **2** before and (b) unstable **2** after irradiation (2 h, λ_{irr} = 365 nm) in CH_2Cl_2 at 20 °C.

light (λ_{irr} = 365 nm), distinct changes in the ^{1}H NMR spectrum are observed, indicating the conversion from stable **2** to unstable **2** and the photostationary state (PSS) was determined: 95:5 unstable **2**/stable **2** in CH_2Cl_2 at 20 °C (see Supporting Information for details).

For self-assembled nanotubes of **2**, a similar characteristic hypsochromic shift was observed as in solution (Figure 4d compared to 4c), indicating that the motor undergoes isomerization, although this may also be due to differences in aggregation as a function of concentration.[74] By virtue of the unique photochemical and thermal stability of molecular motors based on overcrowded alkenes,[53] the long half-life of **2** should allow us to see the different stable and unstable isomers, and any consequential change in morphology of the aggregates.

Changes in Morphology upon Isomerization. As an identical, characteristic hypsochromic shift[46,67,68] was observed in the absorption spectra of nanotubes of **2** (Figure 4c) as for a solution of slow motor **2** (Figure 4d), we investigated morphological changes by cryo-TEM, upon photochemical isomerization of **2** (Figure 9).[75]

After irradiation (10 min, λ_{irr} = 365 nm) of tubes of stable **2** (1:1 with DOPC; total concentration is 1 mg/mL) in water, cryo-TEM revealed that the tubular structures disappear completely, and only vesicles (diameters of 130 nm to micrometers) and pieces of bilayer are observed (Figure 9b). UV−vis absorption measurements on the same sample show a hypsochromic shift upon irradiation of the sample (Figure 10c, from solid to dashed line) that is indicative for the formation of unstable **2**, and we propose that the isomerization of the amphiphilic motor induces the morphological change of the aggregates. Irradiation of toroidal nanotubes of **1** did not lead to a change in their morphology although the molecular motor is capable of isomerizing from stable **1** to unstable **1** in solution (Figure 5), albeit with a very low thermal half-life for the back-isomerization from unstable **1** to stable **1** (see above). As the structures of **1** and **2** are similar, it is likely that both isomerize in the aggregates as observed for **2**. In light of the above, we conclude that the movement of the molecular motor constituent is not the cause for a change in morphology, but rather the change in packing parameter between the different isomers, which is a combination of volume and length of the

DOI: 10.1021/jacs.5b11318
J. Am. Chem. Soc. 2016, 138, 660−669

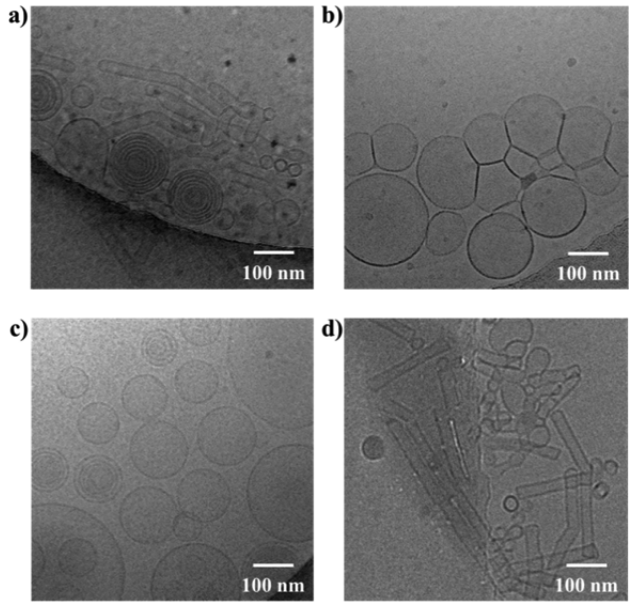

Figure 9. Cryo-TEM microscopy images of coassemblies of amphiphile **2** and DOPC (1:1) in water at a total concentration of 1 mg/mL. The consecutive processes are (a) before irradiation (stable **2**); (b) after irradiation for 15 min at λ_{irr} = 365 nm (unstable **2**); (c) after heating at 50 °C for 16 h (stable **2**); (d) after freeze–thawing 3 times.

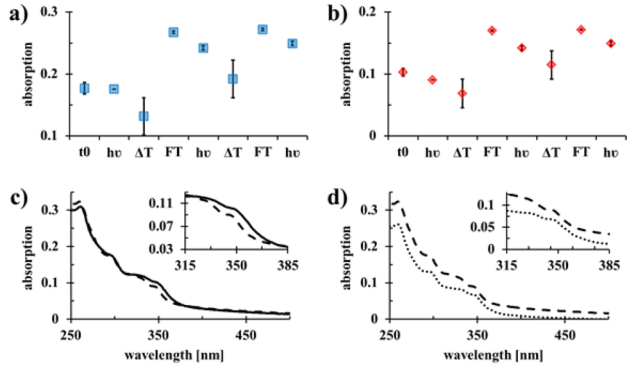

Figure 10. Reversibility of isomerization of coassemblies of **2** and DOPC (1:1) in water at a total concentration of 1 mg/mL. (a) UV–vis absorption maxima at λ = 295 nm (blue squares) and (b) λ = 345 nm (red diamonds). t0 = starting point; hυ = sample irradiated for 10 min at λ = 365 nm; ΔT = sample heated at 50 °C for 16 h; FT = sample freeze–thawed 3 times. (c) Nanotubes of stable **2** with DOPC (1:1) in water (1 mg/mL) before (solid line) and after (dashed line) irradiation (10 min, λ_{irr} = 365 nm; unstable **2**), followed by (d) heating at 50 °C for 16 h (dashed to dotted line; stable **2**). The cycles were performed in triplo. Insets are expanded areas of λ = 315–385 nm.

hydrophobic half and the surface area of the hydrophilic part of an amphiphile.[62,76]

If molecular motor **2** retains its functionality, subsequent warming should induce the thermal isomerization from unstable **2** to stable **2**. After heating the irradiated self-assembled sample (vesicles) at 50 °C for 16 h, however, no change in morphology is observed by cryo-TEM (Figure 9c). This lack of observed change is remarkable as the UV–vis absorption spectrum of the same sample shows a decrease of the absorption over the entire spectrum (Figure 10d, dashed to dotted line), indicating a change in the aggregates.[77]

If given the chance to reorganize, i.e. molecules changing their packing and consequently the morphology of the self-assembled superstructure, we envisioned that the tubes of stable **2** would be reformed from the vesicles. Indeed, upon freeze–thawing the irradiated and subsequently heated sample, the same well-defined tubular structures are reformed (Figure 9d) with identical dimensions (100–200 nm in length, 30 nm in diameter) as in the starting sample, and the absorption spectrum of stable **2** is restored. This is a strong indication that aggregated amphiphilic motor **2** retains its functionality and that isomerization upon irradiation (10 min, λ_{irr} = 365 nm) from stable **2** to unstable **2** causes the nanotubes to change morphology to vesicles, while subsequent thermal back isomerization to stable **2** is responsible for reformation of the nanotubes. This completes the rotary cycle of the amphiphilic molecular motor.

Control Experiments. In order to exclude the possibility that vesicles of unstable **2** reorganize into tubes upon freeze–thawing, we subjected the irradiated sample (vesicles, Figure 9) to freeze–thaw cycles, but no changes in morphology were observed. This confirms that only the stable isomer of the molecular motor forms tubular structures. Furthermore, no changes in morphology could be observed after storing the nanotubes (before irradiation) or vesicles (after irradiation) at room temperature for 24 h in the dark, indicating that the aggregates are stable. As an additional control experiment, in order to exclude the possibility that the change in morphology of the coassemblies is due to DOPC, we irradiated and heated pure DOPC vesicles under identical conditions as the nanotube samples containing the amphiphilic molecular motor. As expected, vesicles consisting of pure DOPC did not change morphology (see Supporting Information Figure S29) when irradiated (15 min, λ_{irr} = 365 nm) or heated (16 h, 50 °C) under identical conditions as the coassemblies of molecular motor **2** and DOPC, providing further evidence that the changes in morphology are a result of the isomerization of the molecular motor. Moreover, we employed energy-dispersive X-ray spectroscopy (EDX) to determine the composition of the vesicles in order to see if they contain both **2** and DOPC. This technique is used for the elemental analysis of a sample and shows the atomic consistence, based on the interaction of different atoms with electron beam excitation,[78] and is used as a qualitative technique to show the presence of certain atoms in the analysis of various soft matter systems.[79−81] As in the mixed samples of **2** and DOPC, phosphorus atoms are present only in DOPC and sulfur atoms are present only in **2**; EDX analysis provides direct evidence for the content of both DOPC and **2** in the vesicles, obtained after irradiation of the nanotubes. The data (see Supporting Information Figure S50) strongly suggest that unstable **2** and DOPC are still mixed after irradiation of the nanotubes, as there are no isolated areas of either **2** (sulfur) or DOPC (phosphorus), and exclude the possibility that the observed vesicles are consisting of pure DOPC.

Reversibility of the System. In order to investigate the reversibility of the changes in morphology, an aqueous solution of nanotubes of stable **2** was irradiated (10 min, λ_{irr} = 365 nm) to induce the stable to unstable isomerization. Then, the aggregates of unstable **2** were heated (50 °C for 16 h) to reform stable **2** and subsequently freeze–thawed.[82] This cycle was repeated three times and in triplo with separate samples, following the absorption at two different wavelengths (λ = 295 and 345 nm), and the results are shown in Figure 10. We

DOI: 10.1021/jacs.5b11318
J. Am. Chem. Soc. 2016, 138, 660–669

studied the morphology of the supramolecular assemblies after each step by cryo-TEM, and the results are shown in Figure 11.

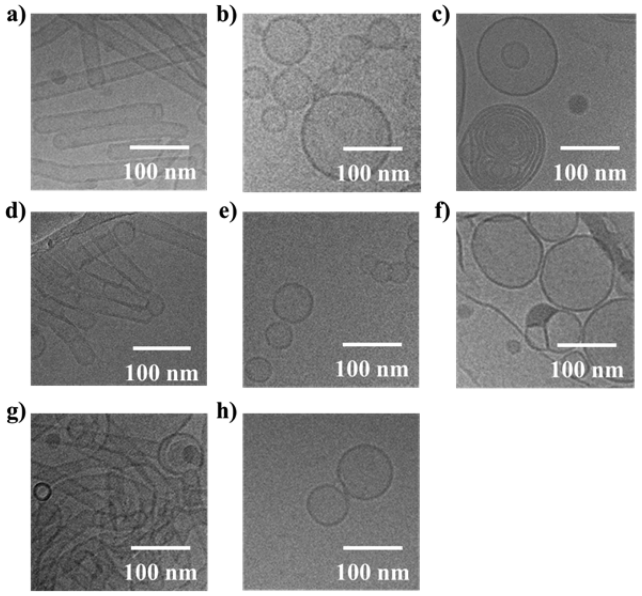

Figure 11. Reversibility of isomerization of coassemblies of **2** and DOPC (1:1) in water by cryo-TEM at a total concentration of 1 mg/mL. In subsequent order: (a) starting point (t0); (b) after irradiation (hυ; 10 min, λ_{irr} = 365 nm); (c) after heating (ΔT; 50 °C, 16 h); (d) after three freeze−thaw cycles (FT); (e) after irradiation (10 min, λ_{irr} = 365 nm); (f) after heating (50 °C, 16 h); (g) after three freeze−thaw cycles; (h) after irradiation (10 min, λ_{irr} = 365 nm).

After confirming the formation of nanotubes from stable **2** (1:1 with DOPC at a total concentration of 1 mg/mL in water) by cryo-TEM (Figure 11a), a UV−vis absorption spectrum was taken and the absorption was measured at two wavelengths: λ = 295 and 345 nm (Figure 10a−b, t0). After irradiation of the nanotubes with UV light (10 min, λ_{irr} = 365 nm), the tubular structures disappeared and only vesicles were observed by cryo-TEM (Figure 11b). The UV−vis absorption spectrum of the aggregates shows the characteristic hypsochromic shift (Figure 10c, solid to dashed line),[46,67,68] indicating the isomerization to unstable **2** and λ_{295} and λ_{345} decrease (Figure 10a−b, hυ). Upon heating, isomerization to stable **2** occurs and λ_{295} and λ_{345} decrease (Figure 10a−b, ΔT and 10d); cryo-TEM shows vesicles (Figure 11c), as before heating (Figure 11b). After freeze−thawing the samples, the nanotube structures are restored (Figure 11d) and λ_{295} and λ_{345} increase significantly (Figure 10a−b, FT). This cycle was repeated three times in triplo, and both cryo-TEM (Figure 11e−h) and UV−vis absorption spectroscopy (Figure 10a−b) show remarkably reproducible and consistent results for the reversible modulation between nanotubes of stable **2** and vesicles of unstable **2** (the absorption spectra after the second and third complete cycle perfectly overlap); the observed behavior is shown schematically in Figure 12. We noticed that the initial nanotubes have a lower absorption than after reformation through irradiation and subsequent heating; however, after the first cycle the UV−vis spectra are identical for the repetitive steps and changes in morphology upon isomerization are highly reproducible.[83] This difference between the first and second cycle is attributed to more efficient packing of these molecules after the first complete cycle or the formation of more aggregates.

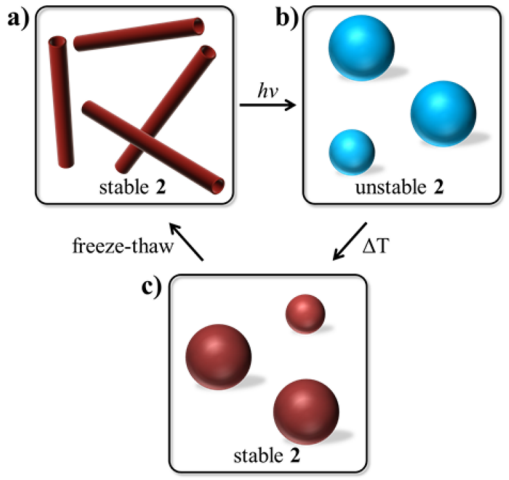

Figure 12. Changes in aggregation upon isomerization of self-assembled molecular motor constituent **2**. (a) Nanotubes of stable **2** which represents the original state of self-assembled stable **2** and can be reformed by freeze−thawing vesicles of unstable **2**. (b) Vesicles of unstable **2**, formed by irradiation of nanotubes of stable **2**. (c) Vesicles of stable **2**, formed by heating of vesicles of unstable **2**.

As described in Figure 12, irradiation of self-assembled stable **2** induces a change in the morphology from nanotubes to vesicles upon isomerization to unstable **2**. Applying heat causes the molecular motor to isomerize back to stable **2**, without causing an observable change in the morphology of the vesicles. After freeze−thawing the sample, however, the original nanotubes of stable **2** are reformed and this complete cycle can be repeated reproducibly a number of times.

CONCLUSIONS

In summary, we present herein, to the best of our knowledge, the first examples in which a molecular motor forms well-defined aggregated structures in water and in which the molecular component causes a reversible change in morphology when exposed to external stimuli. Fast (**1**) and slow (**2**) amphiphilic molecular motors were designed and studied using cryo-electron microscopy and UV−vis spectroscopy. Amphiphile **1** forms toroided nanotubes when coassembled with DOPC in water and, with a half-life of 40 ns as determined by transient absorption spectroscopy, has a theoretical rotation speed of 10 MHz at room temperature, making it one of the fastest molecular motors reported to date. Therefore, its half-life is too short to observe any changes in the aggregates upon irradiation of the motor. Slow molecular motor **2** self-assembles into straight nanotubes in water, and upon irradiation with light, isomerization of the molecular component from stable **2** to unstable **2** causes the tubular structures to reorganize into vesicles. Heating the system induces the isomerization of the molecular motor from unstable **2** to stable **2**, and the nanotubes are subsequently reformed. For the first time, we have shown how a molecular motor retains its function in water and we furthermore demonstrated how isomerization of the molecular constituent in well-defined self-assembled nanotubes causes reorganization into vesicles on-demand in a fully controlled and reversible manner. The results presented in this work could provide access to a new generation of water-soluble molecular machines and offer ample opportunity to couple light-driven

DOI: 10.1021/jacs.5b11318
J. Am. Chem. Soc. 2016, 138, 660−669

motor function to dynamic aggregation, arriving ultimately at responsive supramolecular nanosystems. Current work in our laboratories is aiming to implement a next generation of amphiphilic and water-soluble molecular motors that bear an asymmetric lower half so that the motors have four distinct isomers that may be selectively addressed.

■ ASSOCIATED CONTENT

Supporting Information

The Supporting Information is available free of charge on the ACS Publications website at DOI: 10.1021/jacs.5b11318.

Experimental details, ^{1}H and ^{13}C NMR spectra, raw cryo-TEM images, control experiments, photostationary state determination, details of transient absorption measurements, and EDX (PDF)

■ AUTHOR INFORMATION

Corresponding Author

*b.l.feringa@rug.nl

Present Addresses

†Department of Chemistry, Humboldt-Universität zu Berlin, Brook-Taylor-Straße 2, 12489 Berlin, Germany.

‡Nanochemistry Laboratory, ISIS and icFRC, Université de Strasbourg and CNRS, 8 allée Gaspard Monge, 67000 Strasbourg, France.

Author Contributions

§D.J.v.D. and J.C. contributed equally.

Notes

The authors declare no competing financial interest.

■ ACKNOWLEDGMENTS

We thank Prof. W. R. Browne and Dr. W. Szymański for discussions. This work was supported by the European Research Council (Advanced Investigator Grant 227897; B.L.F.) and the Ministry of Education, Culture and Science of The Netherlands (Gravitation Program 024.001.035; B.L.F.).

■ REFERENCES

(1) Steed, J. W.; Gale, P. A. *Supramolecular Chemistry: From Molecules to Nanomaterials, Vol. 6: Supramolecular Materials Chemistry*; John Wiley & Sons, Ltd.: Weinheim, Germany, 2012.

(2) For a concise review, see: Aida, T.; Meijer, E. W.; Stupp, S. I. *Science* **2012**, *335*, 813−817.

(3) For a perspective, see: Stupp, S. I.; Palmer, L. C. *Chem. Mater.* **2014**, *26*, 507−518.

(4) Verma, G.; Hassan, P. A. *Phys. Chem. Chem. Phys.* **2013**, *15*, 17016−17028.

(5) Zhang, M.; Yan, X.; Huang, F.; Niu, Z.; Gibson, H. W. *Acc. Chem. Res.* **2014**, *47*, 1995−2005.

(6) Zheng, B.; Wang, F.; Dong, S.; Huang, F. *Chem. Soc. Rev.* **2012**, *41*, 1621−1636.

(7) Isaacs, L. *Acc. Chem. Res.* **2014**, *47*, 2052−2062.

(8) Whitesides, G. M.; Boncheva, M. *Proc. Natl. Acad. Sci. U. S. A.* **2002**, *99*, 4769−4774.

(9) Lehn, J.-M. *Top. Curr. Chem.* **2011**, *322*, 1−32.

(10) Lehn, J.-M. *Angew. Chem., Int. Ed.* **2013**, *52*, 2836−2850.

(11) Boyle, M. M.; Smaldone, R. A.; Whalley, A. C.; Ambrogio, M. W.; Botros, Y. Y.; Stoddart, J. F. *Chem. Sci.* **2011**, *2*, 204−210.

(12) Yagai, S.; Kitamura, A. *Chem. Soc. Rev.* **2008**, *37*, 1520−1529.

(13) Velema, W. A.; Stuart, M. C. A.; Szymanski, W.; Feringa, B. L. *Chem. Commun.* **2013**, *49*, 5001−5003.

(14) Tabor, R. F.; Pottage, M. J.; Garvey, C. J.; Wilkinson, B. L. *Chem. Commun.* **2015**, *51*, 5509−5512.

(15) Willerich, I.; Gröhn, F. *Angew. Chem., Int. Ed.* **2010**, *49*, 8104−8108.

(16) Kageyama, Y.; Tanigake, N.; Kurokome, Y.; Iwaki, S.; Takeda, S.; Suzuki, K.; Sugawara, T. *Chem. Commun.* **2013**, *49*, 9386−9388.

(17) Hamada, T.; Sugimoto, R.; Vestergaard, M. C.; Nagasaki, T.; Takagi, M. *J. Am. Chem. Soc.* **2010**, *132*, 10528−10532.

(18) Hosono, N.; Kajitani, T.; Fukushima, T.; Ito, K.; Sasaki, S.; Takata, M.; Aida, T. *Science* **2010**, *330*, 808−811.

(19) Higashiguchi, K.; Taira, G.; Kitai, J.; Hirose, T.; Matsuda, K. *J. Am. Chem. Soc.* **2015**, *137*, 2722−2729.

(20) Yagai, S.; Iwai, K.; Karatsu, T.; Kitamura, A. *Angew. Chem., Int. Ed.* **2012**, *51*, 9679−9683.

(21) Zhang, J.; Jin, J.; Zou, L.; Tian, H. *Chem. Commun.* **2013**, *49*, 9926−9928.

(22) van Herpt, J. T.; Areephong, J.; Stuart, M. C. A.; Browne, W. R.; Feringa, B. L. *Chem. - Eur. J.* **2014**, *20*, 1737−1742.

(23) Hirose, T.; Irie, M.; Matsuda, K. *Adv. Mater.* **2008**, *20*, 2137−2141.

(24) Klajn, R. *Chem. Soc. Rev.* **2014**, *43*, 148−184.

(25) De Sousa, F. B. D.; Guerreiro, J. D. T.; Ma, M.; Anderson, D. G.; Drum, C. L.; Sinisterra, R. D.; Langer, R. *J. Mater. Chem.* **2010**, *20*, 9910−9917.

(26) Florea, L.; Scarmagnani, S.; Benito-Lopez, F.; Diamond, D. *Chem. Commun.* **2014**, *50*, 924−926.

(27) Liu, Y.; Fan, M.; Zhang, S.; Yao, J. *J. Phys. Org. Chem.* **2007**, *20*, 884−887.

(28) Zhang, Q.; Qu, D.-H.; Ma, X.; Tian, H. *Chem. Commun.* **2013**, *49*, 9800−9802.

(29) Ma, X.; Tian, H. *Acc. Chem. Res.* **2014**, *47*, 1971−1981.

(30) Zhang, Q.; Qu, D.-H.; Wu, J.; Ma, X.; Wang, Q.; Tian, H. *Langmuir* **2013**, *29*, 5345−5350.

(31) Xing, P.; Chen, H.; Bai, L.; Zhao, Y. *Chem. Commun.* **2015**, *51*, 9309−9312.

(32) Göstl, R.; Hecht, S. *Chem. - Eur. J.* **2015**, *21*, 4422−4427.

(33) Özçoban, C.; Halbritter, T.; Steinwand, S.; Herzig, L.-M.; Kohl-Landgraf, J.; Askari, N.; Groher, F.; Fürtig, B.; Richter, C.; Schwalbe, H.; Suess, B.; Wachtveitl, J.; Heckel, A. *Org. Lett.* **2015**, *17*, 1517−1520.

(34) Zou, Y.; Yi, T.; Xiao, S.; Li, F.; Li, C.; Gao, X.; Wu, J.; Yu, M.; Huang, C. *J. Am. Chem. Soc.* **2008**, *130*, 15750−15751.

(35) London, G.; Chen, K.-Y.; Carroll, G. T.; Feringa, B. L. *Chem. - Eur. J.* **2013**, *19*, 10690−10697.

(36) Chen, K.-Y.; Ivashenko, O.; Carroll, G. T.; Robertus, J.; Kistemaker, J. C. M.; London, G.; Browne, W. R.; Rudolf, P.; Feringa, B. L. *J. Am. Chem. Soc.* **2014**, *136*, 3219−3224.

(37) Jiang, W.; Wang, G.; He, Y.; Wang, X.; An, Y.; Song, Y.; Jiang, L. *Chem. Commun.* **2005**, *28*, 3550−3552.

(38) Eelkema, R.; Pollard, M. M.; Vicario, J.; Katsonis, N.; Ramon, B. S.; Bastiaansen, C. W. M.; Broer, D. J.; Feringa, B. L. *Nature* **2006**, *440*, 163.

(39) Kudernac, T.; Ruangsupapichat, N.; Parschau, M.; Maciá, B.; Katsonis, N.; Harutyunyan, S. R.; Ernst, K.-H.; Feringa, B. L. *Nature* **2011**, *479*, 208−211.

(40) Li, Q.; Fuks, G.; Moulin, E.; Maaloum, M.; Rawiso, M.; Kulic, I.; Foy, J. T.; Giuseppone, N. *Nat. Nanotechnol.* **2015**, *10*, 161−165.

(41) Wang, J.; Feringa, B. L. *Science* **2011**, *331*, 1429−1432.

(42) Wezenberg, S. J.; Vlatković, M.; Kistemaker, J. C. M.; Feringa, B. L. *J. Am. Chem. Soc.* **2014**, *136*, 16784−16787.

(43) Browne, W. R.; Feringa, B. L. *Nat. Nanotechnol.* **2006**, *1*, 25−35.

(44) Pollard, M. M.; Klok, M.; Pijper, D.; Feringa, B. L. *Adv. Funct. Mater.* **2007**, *17*, 718−729.

(45) Kulago, A. A.; Mes, E. M.; Klok, M.; Meetsma, A.; Brouwer, A. M.; Feringa, B. L. *J. Org. Chem.* **2010**, *75*, 666−679.

(46) Klok, M.; Boyle, N.; Pryce, M. T.; Meetsma, A.; Browne, W. R.; Feringa, B. L. *J. Am. Chem. Soc.* **2008**, *130*, 10484−10485.

(47) Vicario, J.; Meetsma, A.; Feringa, B. L. *Chem. Commun.* **2005**, *47*, 5910−5912.

(48) Koumura, N.; Geertsema, E. M.; van Gelder, M. B.; Meetsma, A.; Feringa, B. L. *J. Am. Chem. Soc.* **2002**, *124*, 5037−5051.

(49) Bauer, J.; Hou, L.; Kistemaker, J. C. M.; Feringa, B. L. *J. Org. Chem.* **2014**, *79*, 4446−4455.
(50) van Delden, R. A.; ter Wiel, M. K. J.; Pollard, M. M.; Vicario, J.; Koumura, N.; Feringa, B. L. *Nature* **2005**, *437*, 1337−1340.
(51) Chen, K.-Y.; Wezenberg, S. J.; Carroll, G. T.; London, G.; Kistemaker, J. C. M.; Pijper, T. C.; Feringa, B. L. *J. Org. Chem.* **2014**, *79*, 7032−7040.
(52) Chen, J.; Chen, K.-Y.; Carroll, G. T.; Feringa, B. L. *Chem. Commun.* **2014**, *50*, 12641−12644.
(53) Feringa, B. L. *Acc. Chem. Res.* **2001**, *34*, 504−513.
(54) Koumura, N.; Zijlstra, R. W. J.; van Delden, R. A.; Harada, N.; Feringa, B. L. *Nature* **1999**, *401*, 152−155.
(55) Geertsema, E. M.; van der Molen, S. J.; Martens, M.; Feringa, B. L. *Proc. Natl. Acad. Sci. U. S. A.* **2009**, *106*, 16919−16924.
(56) Valdes-Aguilera, O.; Neckers, D. C. *Acc. Chem. Res.* **1989**, *22*, 171−177.
(57) Fink, R. F.; Seibt, J.; Engel, V.; Renz, M.; Kaupp, M.; Lochbrunner, S.; Zhao, H.-M.; Pfister, J.; Würthner, F.; Engels, B. *J. Am. Chem. Soc.* **2008**, *130*, 12858−12859.
(58) Kaiser, T. E.; Wang, H.; Stepanenko, V.; Würthner, F. *Angew. Chem., Int. Ed.* **2007**, *46*, 5541−5544.
(59) Feringa, B. L. *J. Org. Chem.* **2007**, *72*, 6635−6652.
(60) Coleman, A. C.; Beierle, J. M.; Stuart, M. C. A.; Maciá, B.; Caroli, G.; Mika, J. T.; van Dijken, D. J.; Chen, J.; Browne, W. R.; Feringa, B. L. *Nat. Nanotechnol.* **2011**, *6*, 547−552. Note that, in this system, irradiation of the bis-thioxanthylidine amphiphile led to *irreversible* cyclization and morphological changes.
(61) Coleman, A. C.; Areephong, J.; Vicario, J.; Meetsma, A.; Browne, W. R.; Feringa, B. L. *Angew. Chem., Int. Ed.* **2010**, *49*, 6580−6584.
(62) Israelachvili, J. N.; Mitchell, D. J.; Ninham, B. W. *J. Chem. Soc., Faraday Trans. 2* **1976**, *72*, 1525−1568.
(63) Hill, J. P.; Jin, W. S.; Kosaka, A.; Fukushima, T.; Ichihara, H.; Shimomura, T.; Ito, K.; Hashizume, T.; Ishii, N.; Aida, T. *Science* **2004**, *304*, 1481−1483.
(64) Jin, W.; Fukushima, T.; Niki, M.; Kosaka, A.; Ishii, N.; Aida, T. *Proc. Natl. Acad. Sci. U. S. A.* **2005**, *102*, 10801−10806.
(65) Barton, D.; Willis, B. *J. Chem. Soc., Perkin Trans. 1* **1972**, 305−310.
(66) Buter, J.; Wassenaar, S.; Kellogg, R. M. *J. Org. Chem.* **1972**, *37*, 4045−4060.
(67) Klok, M.; Janssen, L. P.; Browne, W. R.; Feringa, B. L. *Faraday Discuss.* **2009**, *143*, 319−334.
(68) ter Wiel, M. K. J.; Vicario, J.; Davey, S. G.; Meetsma, A.; Feringa, B. L. *Org. Biomol. Chem.* **2005**, *3*, 28−30.
(69) Full-size cryo-TEM images are provided in the Supporting Information; Figures S30−S47.
(70) Chen, D.; Santore, M. M. *Biochim. Biophys. Acta, Biomembr.* **2014**, *1838*, 2788−2797.
(71) Extrusion of the mixture did not lead to different morphologies. All other samples were not extruded.
(72) Apart from nanotubes, a multilamellar vesicle (MLV) can be seen in the top of Figure 3c. This is a spherical vesicle, most likely from DOPC that is phase separated out.
(73) Xu, H.; Wang, Y.; Ge, X.; Han, S.; Wang, S.; Zhou, P.; Shan, H.; Zhao, X.; Lu, J. R. *Chem. Mater.* **2010**, *22*, 5165−5173.
(74) Rodler, F.; Schade, B.; Jäger, C. M.; Backes, S.; Hampel, F.; Böttcher, C.; Clark, T.; Hirsch, A. *J. Am. Chem. Soc.* **2015**, *137*, 3308−3317.
(75) As the PSS of **2** is very high (95:5), we believe that effects on the morphology due to the presence of small amounts of the other isomer are negligible.
(76) Nagarajan, R. *Langmuir* **2002**, *18*, 31−38.
(77) Viseu, M. I.; Tatikolov, A. S.; Correia, R. F.; Costa, S. M. B. *J. Photochem. Photobiol., A* **2014**, *280*, 54−62.
(78) Goldstein, J.; Newbury, D. E.; Joy, D. C.; Lyman, C. E.; Echlin, P.; Lifshin, E.; Sawyer, L.; Michael, J. R. *Scanning Electron Microscopy and X-ray Microanalysis*, 3rd ed.; New York, USA, 2003.
(79) Jiao, T.; Liu, M. *Thin Solid Films* **2005**, *479*, 269−276.
(80) Meadows, P. J.; Dujardin, E.; Hall, S. R.; Mann, S. *Chem. Commun.* **2005**, *29*, 3688−3690.
(81) Reches, M.; Gazit, E. *Science* **2003**, *300*, 625−627.
(82) Due to the symmetry of the lower-half of **2**, the stable *trans* and *cis* isomers, as well as the unstable *trans* and *cis* isomers, are identical.
(83) We postulate that the lower intensity of the initial spectra (Figure 10a−b, t0) is due to more efficient packing after the nanotubes have been disassembled and reassembled once, although a change in DOPC content or the amphiphilic motor in the nanotubes after the first cycle cannot be excluded.

DOI: 10.1021/jacs.5b11318
J. Am. Chem. Soc. 2016, 138, 660−669